ELSEVIER

Journal of Hazardous Materials 52 (1997) 223–236

JOURNAL OF HAZARDOUS MATERIALS

Early containment of high-alkaline solution simulating low-level radioactive waste in blended cement

R.A. Olson [a,*], P.D. Tennis [a], D. Bonen [a], H.M. Jennings [a], T.O. Mason [a], B.J. Christensen, A.R. Brough [a], G.K. Sun [b], J.F. Young [b]

[a] *Center for Advanced Cement-Based Materials, Northwestern University, 2145 N. Sheridan Rd., Evanston, IL 60208, USA*

[b] *Center for Advanced Cement-Based Materials, University of Illinois at Urbana–Champaign, 204 Ceramics Building, 105 S. Goodwin, Urbana, IL 61801, USA*

Abstract

Portland cement blended with fly ash and attapulgite clay was mixed with high-alkaline solution simulating low-level radioactive waste at a one-to-one weight ratio. The pastes were adiabatically and isothermally cured at various temperatures and analyzed for phase composition, total alkalinity, pore solution chemistry, and transport properties as measured by impedance spectroscopy.

The total alkalinity is characterized by two main drops. The early one corresponds to a rapid removal of phosphorus, aluminum, sodium, and to a lesser extent potassium from the pore solution. The second drop from about 10 h to 3 days is mainly associated with the removal of aluminum, silicon, and sodium. Thereafter, the total alkalinity continues to decrease, but at a lower rate.

All pastes display a rapid loss in fluidity that is attributed to an early precipitation of hydrated products. Hemicarbonate appears as early as 1 h after mixing and is probably followed by apatite precipitation. The hemicarbonate is unstable, however, and decomposes at a rate that is inversely related to the curing temperature. At high temperatures, a sodalite-type zeolite appears at about 10 h after mixing. At 30 days the stabilized crystalline composition includes zeolite, apatite and other minor amounts of $CaCO_3$, quartz, and monosulfate.

The impedance behavior correlates with the pore solution chemistry and X-ray diffraction data. The normalized conductivity of the pastes displays an early drop followed by a large decrease from about 12 h to 3 days. At 3 days the permeability of the cement-based waste as calculated by

* Corresponding author.

PII S0304-3894(96)01809-2

the Katz–Thompson equation is over three orders of magnitude lower than that of Ordinary Portland cement paste. A further decrease in the calculated permeability is not apparent. This particular cement-based system provides rapid stabilization/solidification of the waste material. The transport of waste species is reduced by probable incorporation into apatite, zeolite, and other solid phases. © 1997 Elsevier Science B.V.

Keywords: Blended cement; Containment; High-alkaline solution; Low-level radioactive waste

1. Introduction

Stabilization/solidification of hazardous waste has become a major concern in the modern industrial society due to growing public awareness coupled with restrictive environmental regulations governing waste disposal. Cement-based systems are favored for waste containment because cement-based waste forms set at ambient conditions and have low permeability. They are also inexpensive, nonflammable, and considered as durable.

Immobilization of waste in cement-based materials is related to three mechanisms, (a) physical containment, (b) absorption or chemisorption of cations on the large surface area within the paste, and (c) chemical immobilization through deposition and ion substitution [1,2]. Mature Portland cement paste has a large B.E.T. surface area (about 200 $m^2 g^{-1}$ as measured by nitrogen) that is attributed to the tortuous and interconnected ink-bottle pores that decrease the transport properties of the paste. Blended cement pastes (e.g. cement paste containing pozzolanic materials) usually display lower permeabilities than do plain Portland cement pastes [3]. The high alkalinity characteristic of cement-based materials is favorable for precipitation of many hazardous metals as hydroxides, such as americium [4], cadmium, and nickel [1]. Sulfates, sulfides, phosphates, and carbonates are also typically stable in cement paste [2].

Considerable research effort has been aimed at formulating blended cement for immobilization of low-level radioactive waste. A specific cement blend was recently developed at Pacific Northwest Laboratory for containment of the low-level radioactive waste currently stored at the Hanford site [5]. This cement blend (68% class F fly ash, 21% type I/II Portland cement, and 11% attapulgite clay by mass) was engineered to meet a wide range of specifications involving pumpability, bleeding, toxicity, compressive strength, low heat of hydration, leachability, irradiation, thermal conductivity, curing time, and expansion. Recent studies conducted on mixtures of this blend with simulated Hanford waste have displayed rapid setting and the precipitation of zeolite phases [6]. Zeolites are hydrous aluminosilicates that may facilitate a greater uptake of hazardous species into their lattices due to their high ion exchange capacity. Zeolite formation has been observed in fly ash blended cement pastes at high temperature and high alkalinity [7].

As part of a larger research effort aimed at stabilizing the volatile materials from the off-gas system of the low-level waste disposal vitrification facility, the objective of this research is to characterize the cement-based waste system and evaluate its transport properties, i.e. the decrease in diffusivity and permeability over time as measured by impedance spectroscopy.

2. Concepts of impedance spectroscopy

Impedance spectroscopy (IS) is a non-destructive electrical analysis technique that is used to characterize the microstructure of hydrating cement paste [8–11]. An alternating current is applied to a cement paste specimen and the impedance is measured as a function of frequency. The impedance data are then used to calculate the conductivity and dielectric constant of the paste. The concentration of the pore solution changes with time, so the conductivity of the paste must be normalized by the pore fluid conductivity. The normalized conductivity (σ/σ_0) is a microstructural parameter that depends on the pore size and tortuosity of the pore network and is defined as:

$$\sigma/\sigma_0 = \phi_0 \beta \tag{1}$$

where σ = conductivity of the paste ($S\,m^{-1}$), σ_0 = conductivity of the pore fluid ($S\,m^{-1}$), ϕ_0 = volume fraction of capillary porosity, and β = a unitless connectivity factor [8,12]. The normalized conductivity decreases with hydration as the pore volume decreases and the tortuosity increases.

The normalized conductivity of the paste is directly related to the normalized diffusivity through the Nernst–Einstein equation:

$$D/D_0 = (\sigma/\sigma_0) \tag{2}$$

where D is the diffusivity of the ion in the paste ($m^2\,s^{-1}$) and D_0 is the intrinsic diffusivity in pure water [8,13]. The normalized conductivity is also related to permeability by the Katz–Thompson equation:

$$K = (1/226)(d_c)^2(\sigma/\sigma_0) \tag{3}$$

where d_c is the critical pore diameter (m) and K is the permeability coefficient ($m\,s^{-1}$) [12,14]. A reasonable agreement between the permeability derived from IS and mercury intrusion porosimetry (MIP) measurements and values measured by conventional fluid flow techniques was established [8].

The cement paste microstructure can also be characterized by its dielectric response. The distribution of pore sizes and the pore structure can generate extremely high dielectric constants. This behavior is due to a geometrical amplification within the pore network and is explained as follows. Assume a conductive material of thickness b is placed between two plates of a capacitor with a separation L, where the space between each plate and the inserted material is $d/2$. The capacitance is then defined as:

$$C = \varepsilon_{\text{eff}}\varepsilon_0(A/L) = \varepsilon_s\varepsilon_0(A/L - b) = \varepsilon_s\varepsilon_0(A/d) = \varepsilon_s\varepsilon_0(L/d)(A/L) \tag{4}$$

where ε_{eff} is the effective dielectric constant of the capacitor, ε_s is the dielectric constant of the substance between the inserted material and the plates, ε_0 is the permittivity of free space, and A is the area of the electrodes. The effective dielectric constant is then:

$$\varepsilon_{\text{eff}} = \varepsilon_s\varepsilon_0(L/d) \tag{5}$$

which can be quite large depending upon the L/d ratio, referred to as the dielectric amplification factor. Large effective dielectric constants can be obtained if conductive

grains of diameter L are embedded in insulating grain boundaries of thickness d [15]. Based on measurements and modeling, the dielectric amplification factor in cement paste was defined by the capillary pore size (L) and the thickness of C–S–H gel between pores (d) [8–11].

3. Experimental procedure

The formulation of the blended cement is described in Ref. [5]. One kg of the blended cement composed of 21% ASTM Type I/II Portland cement, 68% Class F fly ash, and 11% attapulgite clay (palygorskite-type) by mass was prepared by rotating the mixture in a large plastic cylinder for 16 h. Chemical compositions of the constituents are given in Table 1. The simulated waste solution with composition shown in Table 2 was prepared, constantly stirred, and maintained at 50°C. In order to simulate the temperature profile of the Hanford waste, the cement was added to the solution when the temperature of the latter dropped to 45°C. The dry, blended cement was mixed with the solution at a one-to-one ratio by mass in a Hobart mixer for 2 min stopping once to redistribute the paste with a spatula.

The cement based waste is to be cast into very large, subsurface vaults. In order to analyze the effects of the different curing conditions (which decrease in temperature from the center to the edges of the vault) on the various properties, four curing regimes were tested. Fig. 1 shows the temperature schedule of the samples. The upper curve (sample 4) represents the approximate temperature profile of the cement-based waste cured under adiabatic conditions. Samples 1, 2, and 3 were cured according to this profile to temperatures of 55, 70, and 85°C, respectively, then cured isothermally at the corresponding temperatures. All specimens were well-sealed to prevent moisture loss.

A 3 mm thick polycarbonate cylinder with an inner diameter of 23 mm was used as a sample holder for the IS specimens. Two stainless steel electrodes were placed 6 cm apart inside the cylinder. Impedance was measured using a Hewlett–Packard Model 4192A impedance analyzer. An impedance curve was generated by applying an alternating current at 128 different frequencies in a range from 11 MHz to 5 Hz and measuring

Table 1
Chemical composition of the constituents in the dry cement blend (in wt %)

Oxide	Cement	Fly ash	Attapulgite clay
SiO_2	22.2	46.1	59.7
Al_2O_3	3.24	25.0	9.05
Fe_2O_3	4.24	7.25	3.17
CaO	64.5	8.02	3.13
MgO	1.13	1.81	11.2
K_2O	0.52	0.63	0.83
Na_2O	0.15	4.74	0.07
TiO_2	0.23	4.70	0.42
P_2O_5	0.12	0.42	1.47
SO_3	2.14	0.12	< 0.1

Table 2
Chemical composition of the solution that simulates the low-level waste at Hanford. All chemicals were analytical grade

Compound	Amount ($g l^{-1}$)	Molecular weight ($g mol^{-1}$)	Density ($g cm^{-3}$)
$NaNO_3$	8.58	84.99	2.26
NaOH	74.85	40.00	2.13
$Al(NO_3)_3 \cdot 9H_2O$	128	375.13	
$Na_3(PO_4) \cdot 12H_2O$	74.4	380.12	1.62
$NaNO_2$	36.9	69.00	2.17
Na_2CO_3	36.2	105.99	2.53
KCl	1.83	74.56	1.98
NaCl	2.5	58.44	2.17
$Na_3(C_6H_5O_7) \cdot 2H_2O$	2.5	294.10	
$Na_2B_4O_7$	0.131	201.22	2.37
Na_2SO_4	3.89	142.04	2.68
$Ni(NO_3)_2 \cdot 6H_2O$	0.302	290.81	2.05
$Ca(NO_3)_2 \cdot 4H_2O$	0.438	236.15	1.90
$Na_4(EDTA) \cdot 2H_2O$	1.415	416.21	
$Na_3(HEDTA)$	5.293	380.24	
$HOCH_2COOH$	0.645	76.05	
$Mg(NO_3)_2 \cdot 6H_2O$	0.028	256.41	1.64

the real and imaginary impedance components at each frequency. The resistance and capacitance of each paste were determined by fitting simulated impedance curves to the experimental curve using the method outlined in Boukamp [16]. Further details of measurement and correction processes are given elsewhere [8–10].

Pore solutions were extracted from companion samples using a steel die press following the procedure of Barneyback and Diamond [17]. The conductivity of the extracted pore solution was measured at a temperature corresponding to that at which it was expressed from the paste. Thermal equilibrium was assumed when the conductivity of the solution was constant at 100 kHz. The extracted pore solutions were diluted to 1:100 and measured for concentrations of sodium, potassium, calcium, silicon, sulfur, aluminum, and phosphorus using inductively coupled plasma photospectrometry (Plasma

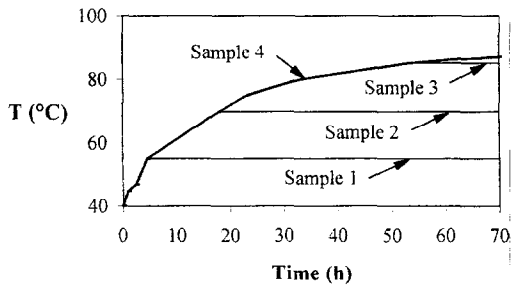

Fig. 1. Temperature schedule for the four different heat treatments. The heavy solid line is the temperature schedule that simulates the actual adiabatic temperature rise.

40, Perkin–Elmer). Additionally, the diluted pore solutions were titrated with 0.5 M HNO_3 and monitored using a digital pH meter to determine the alkalinity of the solution. X-ray diffraction (XRD) was carried out in a diffractometer (Philips Electronics) equipped with a graphite monochromator.

MIP measurements were conducted using a porosimeter (Autoscan 33, Quantachrome) capable of pressurizing from ambient to 33 000 psi. Samples were solvent replaced with methanol for 1 day, then D-dried for at least 2 days before testing. The critical pore diameter (d_c in Eq. (3)) was taken as the inflection point in the total intruded volume vs. diameter curve or the maximum dV/dP value, as defined by Katz and Thompson [14]. The wetting angle was considered to be 130°.

4. Results and discussion

4.1. Total alkalinity and pore solution composition

Fig. 2 shows the titration curves of the pore solutions extracted at various times from sample set 4. The original waste solution displays a step-like curve with several end points corresponding to the neutralization of different species, e.g. OH^-, NO_2^-, NO_3^-, PO_4^{3-}, and CO_2^{2-} (see Table 2). The pore solution extracted at 0.2 h also produces a step-like curve, but its ionic strength is considerably lower than that of the original waste. By 1 h and onward, the titration curves are S-shaped with a single end point, indicating that OH^- becomes the predominant species governing the pH of the pore fluids.

Fig. 3 shows the continuous decrease of the total alkalinity of the pore fluid with time. The term total alkalinity is defined here as the acid neutralizing capacity titrated down to pH 7 and expressed as OH^- equivalent. A substantial drop in the total alkalinity from about 3.9 to 2.5 M occurs from mixing to 1 h (Fig. 3(a)), probably due to

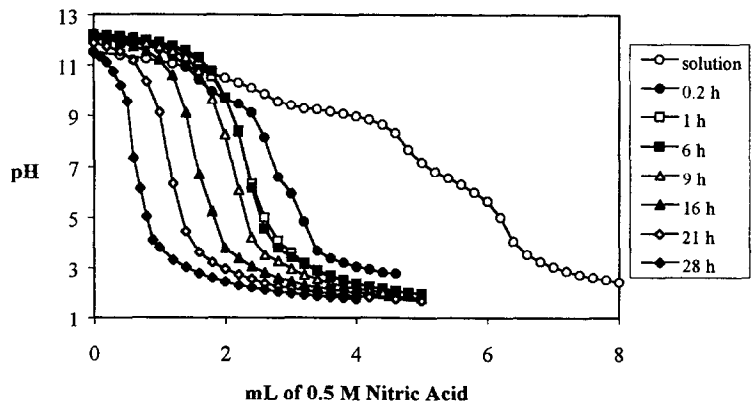

Fig. 2. pH vs. mL HNO_3 used for the titration of the diluted pore solutions extracted from sample set 4. Pore solutions were diluted by 100 using DI water.

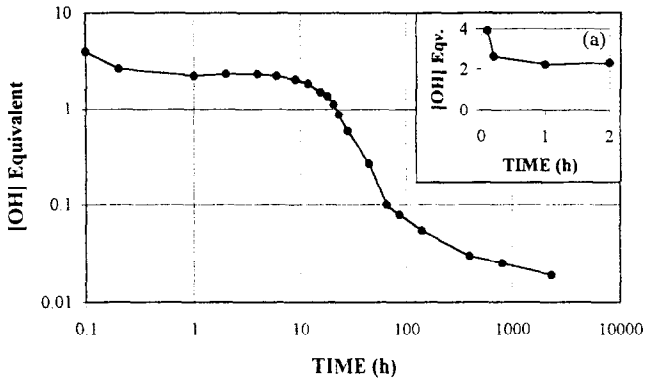

Fig. 3. Total alkalinity vs. time as expressed in terms of [OH] equivalent for the adiabatically cured samples. Fig. 3(a) is the same plot on a linear scale from time 0 to 2 h.

an early removal of P, Al, Na, and K, as shown below. Thereafter, the monotonic decrease in the total alkalinity is followed by a major drop between about 10 and 100 h. A further decrease in the total alkalinity is registered after 3 days, but at a lower rate. The drop from 3.9 to 2.5 M corresponds to a notable decrease in the pH (Fig. 4) and the precipitation of phases produces a significant effect on the impedance spectra.

Phosphorus is almost completely removed from the pore solution within the first 4 h after mixing (Fig. 5). The aluminum concentration behaves similarly, decreasing more than 5-fold at rates directly related to the curing temperature. Sodium shows a greater dependence on temperature. In samples cured at 55°C, only a slight decrease in its concentration was recorded, whereas in the 90°C samples, it drops from about 4000 to 2500 mM. Potassium also decreases during the first 4 h, but at a lower rate. Additionally, the concentrations of the species in the pore solution are affected by the solid phases of the blended cement. Once phosphorus is removed from the original waste solution, there is no other source for it. In contrast, the fly ash, and to a lesser extent the

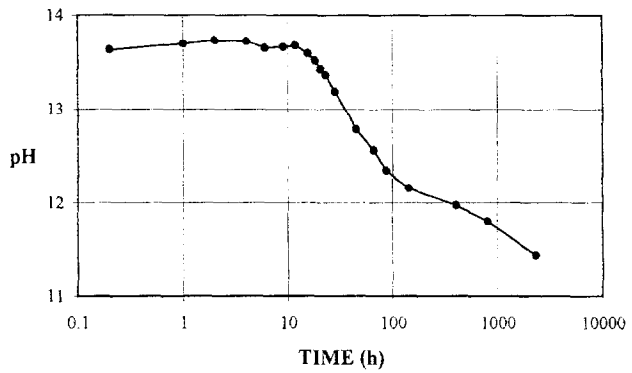

Fig. 4. pH vs. time for extracted pore solution from adiabatically cured samples.

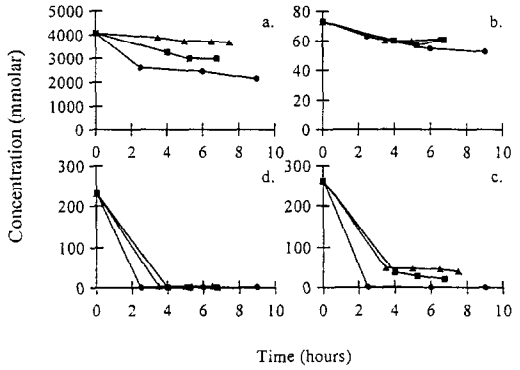

Fig. 5. The concentrations of (a) Na, (b) K, (c) P, and (d) Al for the first 10 h in pore solutions extracted from pastes cured at 55 (▲), 70 (■), and 90° (●) C.

clay, provide a continuous supply of silicon, aluminum, and potassium through dissolution.

Fig. 6 is an illustration of the removal of elements from the pore fluid of the adiabatically cured paste. The second drop in the total alkalinity (Fig. 3) from about 10 h to 3 days corresponds to a decrease of Al^{3+}, Si^{4+}, and Na^{+}, and to a lesser extent S^{6+}. Ca^{2+} and K^{+} concentrations have the lowest rates of decrease. After 3 days, the removal rate of ions from the pore solution slows down considerably.

4.2. Phase composition

In terms of waste immobilization, the Hanford waste has two unfavorable features in addition to the presence of radionucleides: high alkalinity and high temperature. The high temperature is made worse by the exothermic reaction between the waste and the cement, where the temperature at the core of a large monolith can reach 90°C. The high

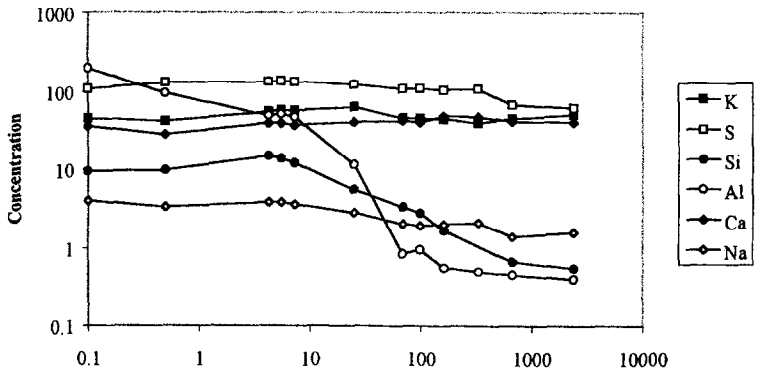

Fig. 6. Concentrations of Na, K, Ca, Al, Si, and S vs. time for the first 2 months in pore solutions extracted from adiabatically cured pastes. All concentrations are given as mmolar except Na, which is molar.

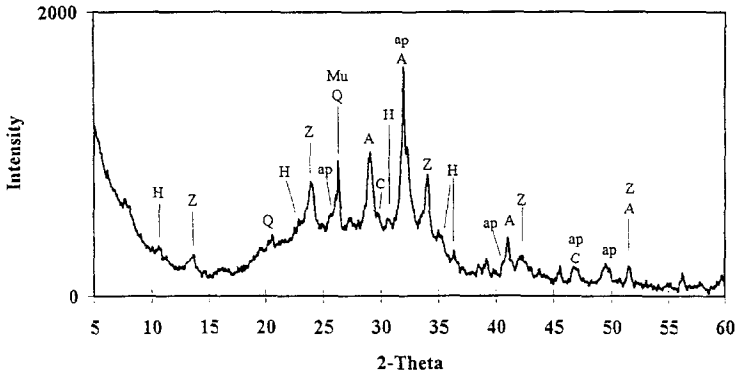

Fig. 7. One day X-ray pattern of the paste cured at 55°C, where A = alite, ap = apatite, C = $CaCO_3$, H = hemicarbonate, Mu = mullite, Q = quartz, and Z = zeolite.

levels of heat and alkalinity in this system generate uncommon hydration products. Brough et al. [6] X-rayed similar pastes cured in a range of 45–90°C and showed that an AFm-type phase (tetracalcium aluminate monosulfate, where another anion can substitute for the sulfate) appears in the paste cured at 45°C 1 h after mixing and a sodalite-type zeolite [18] appears at 1 day. The AFm peak reaches a maximum at 1 day, then decreases to one third of its maximum at 7 days. At higher temperatures in the adiabatically cured paste, the AFm content reaches a maximum at 9 h and disappears at 1 day. The sodalite-type zeolite appears at 9 h and its content steadily increases with time. Katz et al. [19] showed that a significant amount of heat is liberated during the AFm phase formation and that this reaction is a main source of heat generation.

In another set of pastes cured for 30 days at 55, 70, and 90°C, hemicarbonate (tetracalcium aluminate hemicarbonate-12 hydrate or $C_4A\bar{C}_{0.5}H_{12}$) appears in the 1-day X-ray pattern of the specimen cured at 55°C, but is absent from 3 days and on. Fig. 7 shows the corresponding peaks for hemicarbonate (H), sodalite-type zeolite (Z), and a calcium phosphate phase (ap) at 1 day and 55°C. In addition, a significant amount of unreacted clinker minerals including alite (A), quartz (Q), and mullite (M) are present. The calcium phosphate phase closely matches the diffraction pattern of carbonate apatite, however, strong diffractions, especially around its most intense peak at a *d*-spacing of about 2.8 Å, prevent unequivocal identification. Nevertheless, the almost complete removal of phosphorus from the pore solution makes the deposition of apatite or another phosphate phase unavoidable. The effects of age and temperature on the intensity of the apatite peak is anomalous. It appears that its peak height increases to some extent up to 3 days and at higher temperatures, but the latter can equally be related to a better crystallization.

The formation of zeolite is clearly age and temperature dependent. Higher temperatures favor a higher rate of zeolite deposition. Fig. 8 shows that the amount of zeolite increases to some extent up to 30 days. Fraay et al. [20] and Bijen et al. [21] indicated that the rate of fly ash dissolution is related to alkalinity, pH, and temperature, and it is slow below pH 13 and a temperature of 40°C. Large amounts of unreacted fly ash are still observed in this system at 30 days and even 3 months using SEM, so it may be

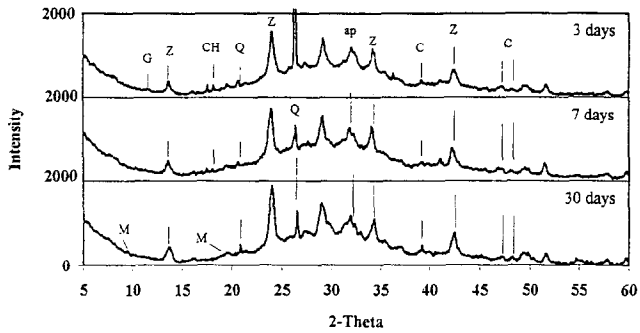

Fig. 8. X-ray patterns of pastes cured at 90°C, where ap = apatite, C = $CaCO_3$, CH = $Ca(OH)_2$, G = gypsum, H = hemicarbonate, M = monosulfate, Q = quartz, and Z = zeolite.

postulated that the dissolution rate of fly ash slows down with time. This is supported by the moderate increase in peak height of zeolite from 3 to 30 days and may also explain the lack of change in the transport properties after 3 days, as is discussed below.

In addition to the phases mentioned, calcite is identifiable in samples with 3 days of curing or more. At 30 days, the phase assemblage includes C–S–H, zeolite, apatite, quartz, and calcite. A small AFm peak appears in samples cured at 90°C and the mullite peak at 3.39 Å is reduced. The former phase probably corresponds to monosulfate and the absence of the latter one may indicate that the crystalline phases of the fly ash have become amorphous. Apatite, zeolite, and monosulfate can incorporate many heavy metals including radioactive ones into their structures. These crystalline compounds may be useful in sequestering potentially toxic or radioactive species in the liquid waste.

4.3. Impedance spectroscopy

Fig. 9 displays the normalized conductivity vs. time for the pastes described above. Although the curing temperature affects the normalized conductivity, the patterns as a

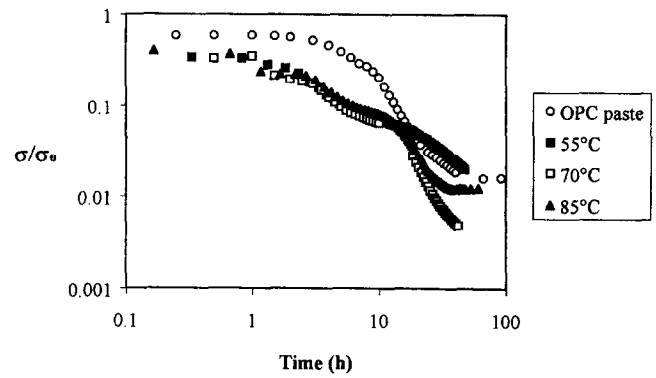

Fig. 9. The normalized conductivity vs. time for the pastes cured at 55, 70, and 85°C and that of plain Portland cement paste with a w/c ratio of 0.5 cured at room temperature.

whole are similar. At 1 h the normalized conductivity drops sharply, indicating a rapid formation of products that results in a decrease and/or disconnection of capillary porosity (Eq. (1)). In comparison to plain Portland cement paste, the normalized conductivity is lower and decreases at a faster rate. This rapid decrease in the normalized conductivity correlates with the rapid setting behavior of these pastes. Rapid flow loss (or stiffening) occurred within the first hour after mixing, which is probably related to the early precipitation of hemicarbonate and apatite.

Several simplified cement-based waste systems were cured isothermally at 85°C for 24 h in order to evaluate the effects of precipitation on the conductivity of the paste. Solutions of NaOH, $Al(NO_3)_3 \cdot 9H_2O$, and $Na_3(PO_4) \cdot 12H_2O$ were mixed with cement and fly ash at a 1:1 ratio by mass. The conductivity at 1 h did not decrease unless $Na_3(PO_4) \cdot 12H_2O$ was added to the mixtures, consistent with the view that phosphate precipitates at 1 h. Hemicarbonate also precipitates at this time as shown by XRD, so both phases play a dominant role in causing a reduction in the fluidity of the paste and an early set.

After the early precipitation of these phases, the normalized conductivity continues to decrease gradually due to the continuous hydration of the cement. The main drop in the normalized conductivity appears after about 12 h of curing and decreases at rates related to the curing temperature (Fig. 9). This drop is most certainly associated with zeolite formation. After 24 h the normalized conductivity is already over an order of magnitude lower than its starting value.

4.4. Permeability

Permeability was calculated via the Katz–Thompson equation (Eq. (3)) using the measured values of the normalized conductivity and the critical pore diameter. Fig. 10 displays the permeability coefficient for hydration times of 3, 7, 14, 28 days, and 3 months for sample set 4 together with calculated values from Christensen et al. [8] and measured values from Nyame and Illston [22,23] and Banthia and Mindess [24] for

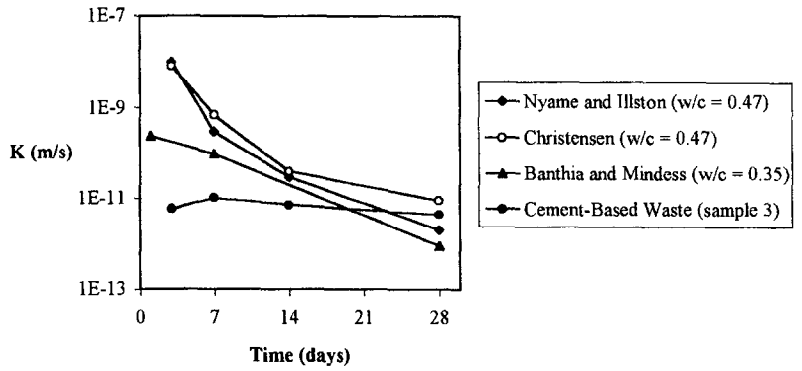

Fig. 10. A comparison of the permeabilities of various cement pastes. The permeability of the cement-based waste was calculated via the Katz–Thompson equation using IS and MIP data.

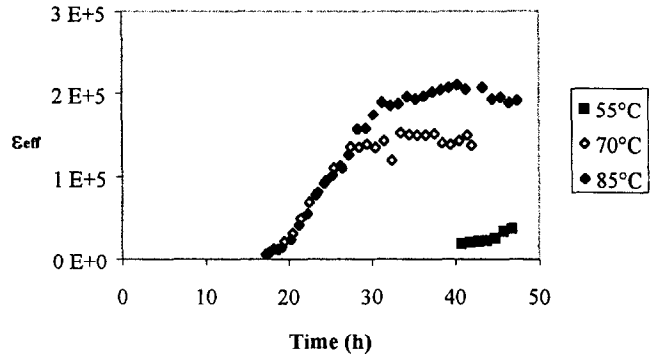

Fig. 11. Effective dielectric constant vs. time for the cement-based wastes cured at 55, 70, and 85°C.

ordinary Portland cement pastes. At 3 days the permeability of the cement-based waste (solution-to-solids ratio of 1.0) is over three orders of magnitude lower than that of Portland cement paste with a w/c ratio of 0.5 and over an order of magnitude lower than cement paste with a w/c ratio of 0.35. Apparently the products formed at early times in the cement-based waste reduce the permeability more effectively than the products in plain Portland cement pastes. Between 3 days and 3 months, the permeability of the cement-based waste remains more or less constant, probably because zeolite precipitation slows down due to the decrease in pH. At 28 days the permeability of the plain cement paste is about the same order of magnitude as the cement-based waste (in the range of 10^{-11} to 10^{-12} m s^{-1}).

4.5. Dielectric amplification

Fig. 11 is a plot of the effective dielectric constant vs. time for the specimens cured at 55, 70, and 85°C. The dielectric constant of the latter two specimens begins increasing at the same time, just after the drop in the normalized conductivity at about 10 h, suggesting that the zeolite phase induces dielectric amplification within the capillary pore network. The extremely high dielectric constants correlate to a high dielectric amplification factor (L/d), which is interpreted microstructurally as large conductive pores embedded in thin boundary layers. The decrease in ε with temperature may correlate with the coarser pore structure created in Portland cement paste when cured at higher temperatures [3], suggesting that the cement waste cured at 55°C has a lower L/d ratio and a more homogeneous microstructure. In contrast to ordinary Portland cement paste, the dielectric constant of the cement waste did not decrease once a maximum dielectric constant was established. The dielectric behavior supports the view that after about 3 days, changes in the pore microstructure are limited.

5. Conclusions

(1) The Hanford waste cement-based system is characterized by an early set due to the deposition of hemicarbonate and apatite. This results in a sharp depletion of the

corresponding ions from the pore solution and a drop of over 66% in the normalized conductivity within the first 4 h.

(2) The combination of high sodium content and high aluminum-bearing ingredients at high temperatures facilitates zeolite precipitation as early as 9 h after mixing. This stage is marked by a prominent decrease in the total alkalinity, pH, and normalized conductivity.

(3) The rapid decrease in the normalized conductivity results in a corresponding decrease in permeability. Even though the normalized conductivity does not drop after 3 days, it is comparable to that of 28-day plain Portland cement paste.

(4) At 28 days, the cement-based waste was found to be composed of naturally occurring minerals such as zeolite, apatite, quartz, and calcite, along with C–S–H and possible minor amount of calcium monosulfate.

(5) The early physical containment and potential for chemical immobilization of the waste is due to the incorporation of elements into apatite, zeolite, and other crystalline structures.

Acknowledgements

This work is supported by the Westinghouse Hanford Company Low-Level Waste Disposal Program. The help of Ash Grove Cement Co., Engelhard Co., and Koch Minerals Co. for supplying materials is greatly appreciated.

References

[1] D. Bonen and S.L. Sarkar, in M.W. Grutzeck and S.L. Sarkar (Eds.), Advances in Cement and Concrete, Proceedings of an Engineering Foundation Conference, New Hampshire, Durham, 24–29 July 1994, American Society of Civil Engineers, 1994, pp. 481–498.
[2] J.R. Conner, Chemical Fixation and Solidification of Hazardous Wastes, Van Nostrand–Reinhold, New York, 1990.
[3] H.F.W. Taylor, Cement Chemistry, Academic Press, London, 1990.
[4] R. Ataback, P. Bouniol, P. Vitorge and P. Lebescop, Cement Concr. Res., 22(2/3) (1992) 419.
[5] R.O. Lokken, P.F.C. Martin and S.E. Palmer, Effects of curing temperature and curing time on double-shell tank waste grouts, Pacific Northwest Laboratory, HGTP-93-0302-01, August 1993.
[6] A. Brough, A. Katz, T. Bakharev, R.J. Kirkpatrick, L.J. Struble and J.F. Young, Mat. Res. Soc. Proc., (1994) in press.
[7] J.L. LaRosa, S. Kwan and M.W. Grutzeck, J. Am. Ceram. Soc., 75(6) (1992) 1574.
[8] B.J. Christensen, R.T. Coverdale, R.A. Olson, S.J. Ford, E.J. Garboczi, T.O. Mason and H.M. Jennings, J. Am. Ceram. Soc., 77 (11) (1994) 2789.
[9] R.T. Coverdale, B.J. Christensen, T.O. Mason, H.M. Jennings, E.J. Garboczi and D.P. Bentz, J. Mater. Sci., 30 (1995) 712.
[10] R.T. Coverdale, B.J. Christensen, T.O. Mason, H.M. Jennings and E.J. Garboczi, J. Mater. Sci., 29 (1994) 4984.
[11] R.A. Olson, B.J. Christensen, R.T. Coverdale, S.J. Ford, E.J. Garboczi, H.M. Jennings and T.O. Mason, J. Mater. Sci., (1995) in press.
[12] E.J. Garboczi, Cement Concr. Res., 20 (4) (1990) 591.
[13] E.J. Garboczi and D.P. Bentz, J. Mater. Sci., 27 (1992) 2083.

[14] A.I. Katz and A.H. Thompson, Phys. Rev. B, 34(11) (1986) 8179.
[15] A.J. Moulson and J.M. Herbert, Electroceramics, Chapman and Hall, New York, 1990, p. 261.
[16] B.A. Boukamp, Equivalent circuit (EQUIVCRT.PAS), University of Twente, Department of Chemical Technology, P.O. Box 217, 7500 AE Enschede, The Netherlands, 1988.
[17] R.S. Barneyback Jr. and S. Diamond, Cement Concr. Res., 11 (1981) 279.
[18] R. von Ballmoos, Collection of Simulated XRD Powder Patterns for Zeolites, Butterworth Scientific, NJ, 1984, pp. 94–95.
[19] A. Katz, A.R. Brough, T. Bakharev, R.J. Kirkpatrick, L.J. Struble, J.F. Young, Mat. Res. Soc. Proc., (1994) in press.
[20] A.L.A. Fraay, J.M. Bijen and Y.M. de Hann, Cement Concr. Res., 19(2) (1989) 235.
[21] J. Bijen and H. Pietersen, in M.W. Grutzeck and S.L. Sarkar (Eds.), Advances in Cement and Concrete, Proceedings of an Engineering Foundation Conference, New Hampshire, Durham, 24–29 July 1994, American Society of Civil Engineers, 1994, pp. 292–327.
[22] B.K. Nyame and J.M. Illston, 7th International Congress of Cement Chemistry, Vol. 3, 1980, VII81–5.
[23] B.K. Nyame and J.M. Illston, Mag. Concr. Res., 33(116) (1981) 139.
[24] N. Banthia and S. Mindess, Cement Concr. Res., 19(5) (1989) 727.